COAL PERMEABILITY AND CRACK DISTRIBUTION CHARACTERISTICS IN UNLOADING CONFINING PRESSURE EXPERIMENTS UNDER DIFFERENT WATER PRESSURES

by

Qiang TAN[a,b], Ru ZHANG[b,c*], Mingzhong GAO[b,c], Qianying LIU[b,c], Zetian ZHANG[b,c], and Zheqiang JIA[b,c]

[a] College of Architecture and Environment, Sichuan University, Chengdu, China
[b] State Key Laboratory of Hydraulics and Mountain River Engineering, Sichuan University, Chengdu, China
[c] College of Water Resource and Hydropower, Sichuan University, Chengdu, China

Original scientific paper
https://doi.org/10.2298/TSCI170310195T

This paper addresses the mechanical behavior and permeability characteristics of the unloading coal under different water pressures in the TOP2518-comprehensive-rock-testing system. With the use of the computed tomography scan tests, the 3-D crack distribution characteristics of the fractured coal are obtained and reconstructed. The difference in the 3-D crack distribution of unloading coal induced by different water pressures is also analyzed in detail. The results show that, as the water pressure changes from 0 MPa to 8 MPa, the peak stress of unloading coal gradually decreases, and that the variation degree of permeability of the coal samples increases significantly comparing with the initial permeability.

Key words: *water pressures, unloading coal, permeability characteristics, crack distribution*

Introduction

Mining activities have leaded to the redistribution of the stress of the underground rock. The coal in excavation-disturbed zones is always subjected to the increasing vertical stress and decreasing horizontal stress, [1]. Due to all coal mining gradually exploring in the deeper areas, there exist high stress and high groundwater pressure in the deep coal seams. The coal production is often accompanied by water spray dust removing, drilling construction, water pressure pre-split, and other water injection measures, *e. g.*, [2]. The poor drainage may lead to the accumulated water in some locations in a coal seam. Under the dual effects of load and fluid pressure, the coal deformation has caused a great change in the crack distribution, which changes the mechanical properties and permeability of coal considerably, [3]. If the mining coal is affected by confined water, it accelerates crack expansion and the formation of new cracks. Thereby, losing the ability to form a water barrier, the entire fracture may occur under the action of water pressure. It may lead to water inrush accidents in coal mines, [4], which causes the considerable economic losses and casualties. Therefore, for coal mine water inrush prevention and forecasting, it is critical to know the distribution of the fracture and the change

* Corresponding author, e-mail: zhangru@scu.edu.cn

in the mechanical properties, and permeability characteristics of mining coal under different water pressures.

Because of the change of the mechanical behavior and permeability characteristics of coal due to the interaction between coal and water, Brace [5] and Bulau *et al.* [6] noted that the synergistic effect of groundwater infiltration and water chemistry aggravates the fissure interaction and crack aggregation deformation effects, which may lead to instability failure of rock mass. The acoustic emission characteristics of coal under different pore water pressures were reported in [7]. The change rule of coal permeability under fluid-solid coupling was discussed in [8]. The evolution of rock permeability with pore pressure and confining pressure is not considered in the real mining conditions of the unloading path, *e. g.*, [9, 10]. For the micro-mechanism changes of crack occurring in the rock caused by rock rupture, a fractal description of joint fracture based on fractal theory was reported in [11, 12]. The distribution regularity of the internal voids in rock by analyzing the difference in the gray value distribution of the computed tomography (CT) scanning images was proposed in [13]. The fracture of rock mass induced by mining pressure and water disturbance stress has been an essential precursor feature of mine water inrush, [14].

With the motivation of the previous idea, our aim of the present paper is to perform the infiltration unloading experiments using a TOP2518-comprehensive-rock-testing system, and to consider the micro-mechanism of damaged coal samples after industrial CT scanning. Moreover, the permeability and crack distribution of unloading coal under different water pressures will be considered to better explain the seepage features of the surrounding rock under mining disturbance, and to evaluate the fracture mode and shape of the mining rock under the action of water pressure.

Methodology

Test method for infiltration unloading of coal

To investigate the changes in the mechanical and seepage characteristics of unloading coal under different water pressures, it is necessary to ensure that the experiment is scientific and pertinent. Thus, it is particularly important to determine the water pressure during the unloading process. The hydraulic pressure of the aquifer measured by boreholes as part of the coal field exploration data is shown in tab. 1, where the typical groundwater pressure of the mine is approximately 2 MPa and the distribution range is 0-4 MPa. A high pressure of 4-8 MPa was detected in the Shanxi Wuyang, Shanxi, Chine coal mine. Therefore, the pressure of the infiltration test during the unloading process was set to 0, 2, 4, and 8 MPa. Considering that deep mining will be the main method for obtaining coal energy in the future and that the current coal mining depth is over 1,000 m, the design depth of this experiment is 1,000 m, and the average height of the overlying strata is set to 0.025 MPa/m, thus, the initial vertical stress and horizontal stress are 25 MPa. In this experiment, the pseudo-triaxial (CTC experiment) loading and unloading scheme is used, the axial pressure is simulated as the support pressure, and the confining pressure is simulated as horizontal stress. To simulate the dynamic behavior of mining coal, the coal mining conditions is simulated by increasing the axial pressure and reducing the confining pressure simultaneously. We applied different seepage pressures on the coal samples during the unloading process. Because the confining pressure must be greater than the seepage pressure, we stopped

Table 1. Statistical results of the head pressure in the aquifer of the Datong coal mine, Datong, China

Water pressure [MPa]	Boreholes
0-1	2
1-2	25
2-3	7
3-4	1

unloading the confining pressure when the confining pressure was 1 MPa larger than the seepage pressure. The stress paths of different seepage pressure unloading test are shown in fig.1. The permeability test is based on the Darcy steady-state method, and the seepage medium is water. The rock sample permeability is defined, according to Darcy's law, by:

$$k = \frac{Q\mu L}{\Delta pA} \tag{1}$$

where k is the permeability of the sample, A – the cross-sectional area of the material through the fluid, Q – the flow rate, μ – viscosity of water, L – the length of the sample, and Δp – the head pressure of the sample.

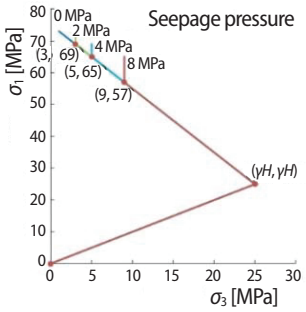

Figure 1. Stress path of unloading coal under different seepage pressures

The infiltration unloading experiment of coal was performed using the TOP2518-rock-comprehensive-testing system illustrated in fig. 2. It has excellent long-term stability and can complete the *high temperature – high pressure – high permeability pressure* multi-field coupling test, as displayed in fig. 3, shows the installation of coal samples in this experiment.

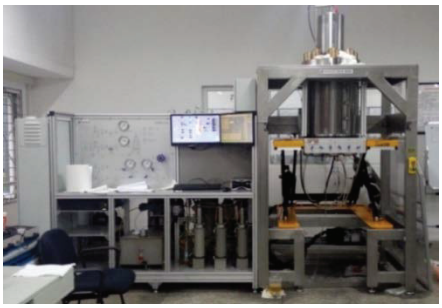

Figure 2. The TOP2518 rock comprehensive testing system

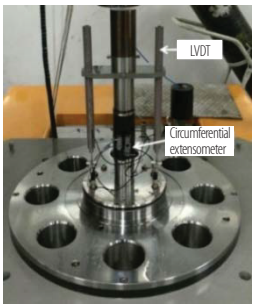

Figure 3. Installation of the coal samples

The CT scanning reconstruction of the crack network

The crack networks of the damaged coal samples are reconstructed after the industrial CT scanning, and the micro-mechanism of the crack distribution is studied. The industrial CT can display the internal structure, composition, material and defect situation in the form of 2-D tomographic images or 3-D images without damage to the detected object, [15]. It can be used to detect the space position, the shape and other information on the micro-cracks in the rock. The physical principle is based on the interaction between the ray and material. When the beam passes through the object, a considerable part of the incident photons turns into the material scattering due to the interaction of photons and matter; thus, the radiation intensity is weakened. After a bundle of initial intensity of, I_0, of the X-ray passing through the material with a thickness, d, the weakened intensity is written:

$$I = I_0 \mathrm{e}^{-\alpha d} \tag{2}$$

where α is the X-ray attenuation coefficient. In eq. (2), α is written:

$$\alpha = \rho\left[\sigma(E) + b\frac{Z^{3.8}}{E^{3.2}}\right] \tag{3}$$

where ρ is the material density, σ – the Klein coefficient related to energy, E – the ray energy, $b = 9.8 \cdot 10^{-24}$, and Z – the effective atomic number.

When the rays pass through a variety of materials, the intensity of the radiation attenuates is the exponential sum of the absorption of different substances, given by:

$$I = I_0 \mathrm{e}^{-\sum \alpha_i d_i} \tag{4}$$

where α_i and d_i are the X-ray attenuation coefficient, and the thickness of the different material, respectively.

When a series of X-ray detectors are installed around the detected substance, the X-ray intensity from different angles can be detected. The cross-sectional analysis of the material failure coefficient can be solved by the eq. (4). Thus, we can construct an image of the scanned object. The attenuation coefficient is typically converted to the CT value λ according to the following equation:

$$\lambda = 1000\frac{\alpha_t - \alpha_w}{\alpha_w} \tag{5}$$

where α_t and α_w are the X-ray attenuation coefficients of the test material, and water, respectively.

Information on the coal structure is obtained in the form of pictures by industrial CT scanning. Because the majority of the cracks in the coal are not filled with solid matter, the cracks are black. The low density material and the initial hole are distributed in the coal sample, and its representation in the image is similar to the cracks caused by the test, which cause hinder the recognition of cracks. The noise contained in the image is removed to enhance the contrast between the crack and the remainder of the image. With the use of the gray value difference between the crack and coal, the MATLAB batch program is used to binarize, stretch and denoise the original CT image, and then, the image is transformed into binarized images. The distribution of point cloud data of the coal samples crack body in the 3-D space is obtained by the CT scanning sequence interval. The 2-D images were reconstructed into 3-D images by importing the processed CT images into Mimics 16.0.

Spatial fractal dimension of fractured coal

Mandelbrot [16] proposed the concept of fractals to express complex images and complex processes. Fractal theory was applied successfully to geotechnical engineering by Xie [12]. The rock joint cracks are rough and have fractal characteristics. Fractal dimensions can accurately characterize the spatial distribution of 3-D crack body. According to the literature [17], the fractal volume measurement of the crack body is:

$$V(\delta_i) = V_0 \delta_i^{3-D} \tag{6}$$

where $V(\delta_i)$ is the measurement volume of the 3-D cracked body, δ_i – the side length of the covering cube, V_0 – the constant related to δ_i, and D – the fractal dimension of the spatial distribution of the 3-D crack.

The 3-D crack body in coal can be considered to consist of the point cloud. The cloud is covered by the cubic covering method, as displayed in fig. 4. The volume of the 3-D crack

body can be approximated as the products of the covering cubic volume and the required cube number.

$$V(\delta_i) = N_i \, \delta_i^3 \tag{7}$$

where N_i is the required cube number.

Substituting eq. (7) into eq. (6) and taking the logarithms of the expressions yields:

$$\lg(N_i) = \lg(V_0) - D\lg(\delta_i) \tag{8}$$

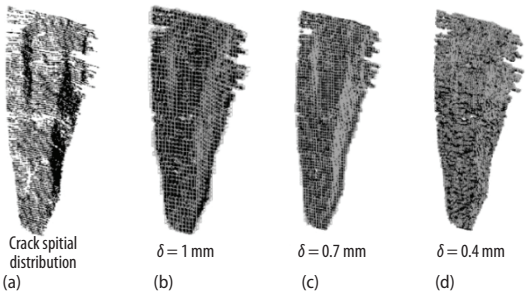

Figure 4. Covering process of 3-D cracks

where D is fractal dimension. The fractal dimension of the spatial distribution of 3-D cracks can be calculated using the cubic covering method. The utility model is advantageous in that the fractal dimensions obtained by this method can reflect the degree of complexity, roughness, orientation, and opening information of 3-D cracks.

Experiment and results

Experimental procedures

The experimental procedures are as follows.

- Saturating the coal: vacuuming the coal samples and then saturating them with water for 48 hour.
- Exerting confining pressure: applying confining pressure up to 25 MPa at a rate of 2 MPa per minute.
- Applying seepage pressure: setting the seepage pressure to 0, 2, 4, and 8 MPa.
- Unloading test: increase the axial pressure and unload the confining pressure for the coal simultaneously with a speed of 2 MPa per minute and 1 MPa per minute. After reaching the peak, switch to the axial displacement control with a loading speed of 0.04 mm per min. The test ends when the coal sample loses the ability to load.

The stress path of the different seepage pressure unloading test is shown in fig.1, the coal sample images before the test is displayed in fig. 5.

Figure 5. The coal samples

Mechanics and seepage characteristics of unloading coal under different water pressures

As illustrated in fig. 6, the curve of the permeability and the stress of typical coal samples can be produced according to the coal infiltration unloading tests under different water pressures. The permeability change law of the coal samples can be divided into three stages:

- Fluctuation stage: the early loading, unloading confining pressure to the coal causes initial micro-cracks to open, and loading axial pressure causes internal micro-cracks to close. The

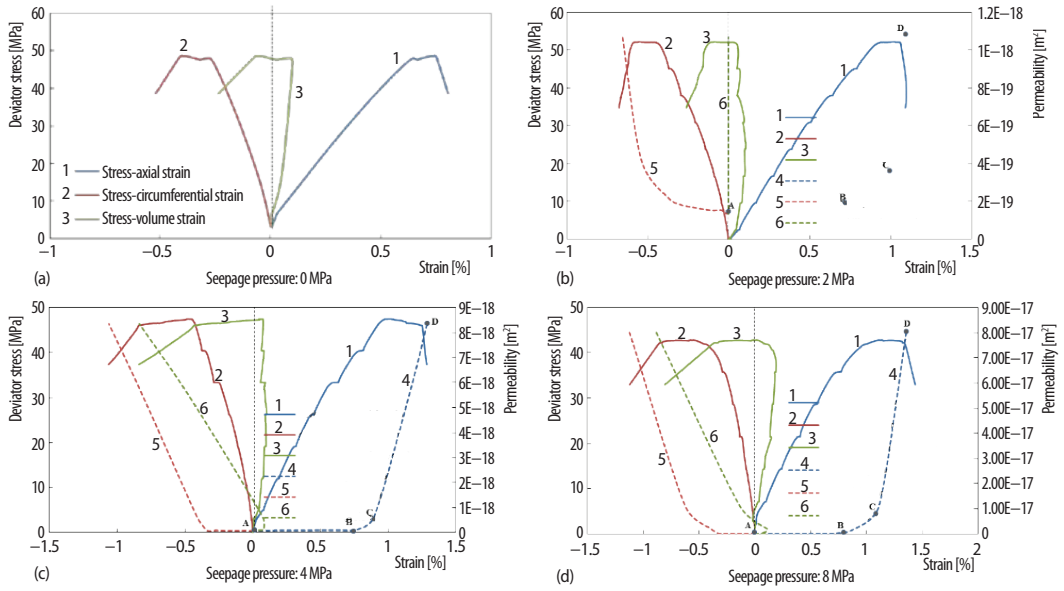

Figure 6. Permeability and stress variation in a typical coal sample unloading process under different water pressures; (b) and (d): *1 – Deviator stress-axial strain, 2 – Deviator stress-circumferential strain, 3 – Deviator stress-volume strain, 4 – Permeability-axial strain, 5 – Permeability-circumferential strain, 6 – Permeability-volume strain* (*for color image see journal web site*)

two actions affect each other, and the permeability of the coal approach the initial permeability.

– Slow rising stage: coal samples from the yield stress area begin to exhibit internal injuries and initial microcracks, which extend the coal dilatancy. The seepage channel increases, and the permeability slowly rises.
– Fast rising stages: The coal damage continues, the stress does not rise considerably, the deformation growth continues in the form of internal macroscopic cracks in the coal samples, and the permeability surges until the end of the test. Contrasting with permeability under different water pressure evolution processes, the coal permeability significantly increased along with the increase in water pressure, the difference in water pressures of 2, 4, and 8 MPa, increased 7.59, 87.73, and 393.74 times, respectively.

A comparison of the mechanical behavior curve of different permeable coals in the unloading process indicates that the peak stress of the coal and the load capacity decrease as the seepage pressure increases. The exponentially functional relationship between the seepage pressure and the peak stress of the coal sample is:

$$\sigma_p = -0.8431\mathrm{e}^{(0.2817p)} + 50.77 \tag{9}$$

where σ_p is the peak stress of coal sample, and p is the seepage pressure.

Spatial fractal dimension of unloading coal fractures under different water pressures

As shown in fig. 7, the surface morphology and crack distribution of the original coal sample and reconstruction model are highly consistent. The cross-crack in the sample

became more complex as the seepage pressure increasing. Only two intersectional cracks occurs when the seepage pressure is 0, 2, and 4 MPa. However, when the seepage pressure increases to 8 MPa, the coal samples are divided into several parts by more complex fractures.

Setting the cube size to 0.25, 0.5, 0.75, 1, 1.25, 1.5, 1.75, 2, and 2.25 mm, the fractal dimensions of 3-D cracks under different water pressures are obtained from eq. (9). The $\log(\delta_i) - \log(N_i)$ curves show good linear correlation, as shown in fig. 8, which illustrate the permeability of the coal unloading of the 3-D crack body space distribution with fractal characteristics. It indicates that the method is reliable. With increasing water pressure, the dismembering of the coal crack is more complex when the fractal dimension is significantly increased.

The exponentially functional relationship between the fractal dimensions of the crack body and the water pressure is:

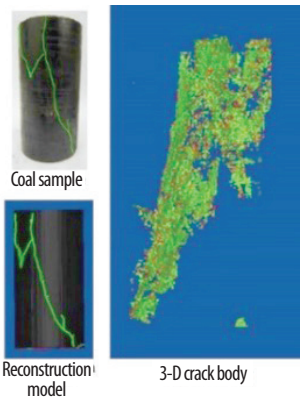

Figure 7. Actual coal sample, reconstruction model and 3-D crack body (seepage pressure: 2 MPa)

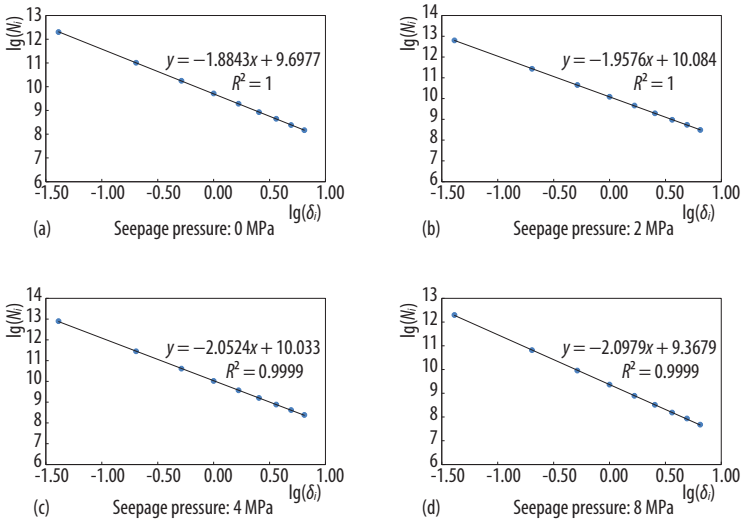

Figure 8. Fractal dimension of the 3-D crack under different water pressures

$$D = -0.2726 \times e^{(-0.2124p)} + 2.152 \tag{10}$$

where D is the fractal dimension of the crack distribution in coal, and p is the seepage pressure.

The obtained results demonstrate that higher seepage pressure lead to a higher rock damage fracture density. Furthermore, a more complex spatial distribution results in a higher degree of the broken coal and higher probability of the water inrush accidents.

Conclusions

In the present work, we obtained the mechanical behaviors and permeability characteristics of the coal considering different water pressures in unloading tests. During the coal

unloading process, the axial, circumferential and volume deformation near the peak stress may exhibit a large deformation platform and the volume expands considerably. The permeability change law can be divided into three stages, *i. e.* fluctuation, slowly rising, and fast rising. Moreover, with the aid of the experimental data, the exponential function relationship between the water pressure and peak stress of the coal was obtained and the evolution of the permeability under different water pressures was compared. The coal crack body induced by unloading tests exhibited fractal characteristics. The obtained results show that, with the increase of the seepage pressure, the fracture distribution complexity of the unloading coal is higher, and in that case, the probability of the causing water inrush accidents is greater. It is of an importantly theoretical and practical significance to handling the real-word problems in coal mining.

Acknowledgment

This work was supported by the National Science Foundation for the Excellent Youth Scholars (No. 51622402).

Nomenclature

A – cross-sectional area of the sample, [m^2]
b – constant, equal to $9.8\cdot10^{-24}$, [–]
D – fractal dimension, [–]
d – material thickness, [m]
d_i – thickness of the different material, [m]
E – ray energy, [eV]
I – weakened intensity of the X-ray, [eV]
I_0 – initial intensity of the X-ray, [eV]
k – permeability of the sample, [m^2]
L – length of the sample, [m]
N_i – the required cube number, [–]
p – seepage pressure, [MPa]
Δp – head pressure of the sample, [MPa]
Q – flow rate, [m^{3}s^{-1}]
V_0 – a constant related to δ_i, [–]
$V(\delta_i)$ – measurement volume of the 3-D cracked body, [mm^3]
Z – effective atomic number, [–]

Greek symbols

α – X-ray attenuation coefficient, [m^{-1}]
α_i – X-ray attenuation coefficient of the different material, [m^{-1}]
α_t – X-ray attenuation coefficients of the test material, [m^{-1}]
α_w – X-ray attenuation coefficients of water, [m^{-1}]
δ_i – side length of the covering cube, [mm]
λ – CT value, [Hu]
μ – viscosity of water, [Pa·s]
ρ – material density, [kgm^{-3}]
σ – Klein coefficient related to energy, [–]
σ_p – peak stress of coal sample, [MPa]

References

[1] Xie, H., *et al*., Mining-Induced Mechanical Behavior in Coal Seams under Different Mining Layouts , *Journal of China Coal Society*, *36* (2011), 7, pp. 1067-1074
[2] Wang, Y., Ma, F., Technology Coal Body Note Water Pressure Splits One Kind Improves Back Production Effective Method of Coal, *Coal Technology*, *25* (2006), 1, pp. 39-41
[3] Wu, Q., *et al*., Numerical Simulation of Lagging Water-Inrush Mechanism of Rock Roadways Near Fault Zone, *Journal of China University of Mining & Technology*, *37* (2008), 6, pp. 780-785
[4] Zhao, S., *et al*., Mechanism Analysis of Water Inrush in Daxing Coal Mine, *Journal of China Coal Society*, *31* (2006), 5, pp. 618-622
[5] Brace, W. F., A Note on Permeability Changes in Geologic Material Due to Stress, *Pure and Applied Geophysics*, *116* (1978), 4, pp. 627-33
[6] Bulau, J. R., *et al*., The Role of Aqueous Fluids in the Internal Friction of Rock, *Journal of Geophysical Research*, *89* (1984), B6, pp. 4207-4212
[7] Wang, X., *et al*., Numerical Simulation of Failure Processes and Acoustic Emissions of Rock Specimen with Imperfections under Different Pore Pressures, *The Chinese Journal of Geological Hazard and Control*, *20* (2009), 2, pp. 52-59
[8] Cheng, Q., *et al*., Evolution Law of the Structure and Permeability for Coal under Solid-Liquid Coupling, *Journal of Mining and Safety Engineering*, *29* (2012), 3, pp. 400-406

[9] Walsh, J. B., Effect of Pore Pressure and Confining Pressure on Fracture Permeability, *International Journal of Rock Mechanics & Mining Sciences & Geomechanics Abstracts*, *18* (1981), 5, pp. 429-435
[10] Yang, Y., *et al*., Test Study on Permeability Properties of Coal Specimen in Complete Stress-Strain Process, *Rock and Soil Mechanics*, *28* (2007), 2, pp.381-385
[11] Lee, Y. H., *et al*., The Fractal Dimension as a Measure of the Roughness of Rock Discontinuity Profiles, *International Journal of Rock Mechanics & Mining Science & Geomechanics Abstracts*, *27* (1990), 6, pp. 453-464
[12] Xie, H., *Fractals in Rock Mechanics*, CRC Press, Boca Raton, Fla., USA, 1993
[13] Peng, R., *et al*., Computation of Fractal Dimension of Rock Pores Based on Gray CT Images, *Science Bulletin*, *56* (2011), 31, pp. 3346-3357
[14] Yang, T., *et al*., State of the Art of Inrush Models in Rock Mass Failure and Developing Trend for Prediction and Forecast of Groundwater Inrush, *Chinese Journal of Rock Mechanics & Engineering*, *26* (2007), 2, pp. 268-277.
[15] Bernard, S., *et al*., Ultrastructural and Chemical Study of Modern and Fossil Sporoderms by Scanning Transmission X-ray Microscopy (STXM), *Review of Palaeobotany and Palynology*, *156* (2009), 1, pp. 248-261
[16] Mandelbrot, B. B., Fractals-a Geometry of Nature, *New Scientist*, *127* (1990), 1734, pp. 38-43
[17] Xie, H., *Introduction to Fractal Rock Mechanics*, Science Press, Beijing, China, 1996

Paper submitted: March 10, 2017
Paper revised: May 1, 2017
Paper accepted: May 26, 2017